Speed Estimation of Induction Motor Using Model Reference Adaptive System with Kalman Filter

Pavel BRANDSTETTER[1], Marek DOBROVSKY[1]

[1]Department of Electronics, Faculty of Electrical Engineering and Computer Science, VSB–Technical University of Ostrava, 17. listopadu 15/2172, 708 33 Ostrava, Czech Republic

pavel.brandstetter@vsb.cz, marek.dobrovsky@vsb.cz

Abstract. *The paper deals with a speed estimation of the induction motor using observer with Model Reference Adaptive System and Kalman Filter. For simulation, Hardware in Loop Simulation method is used. The first part of the paper includes the mathematical description of the observer for the speed estimation of the induction motor. The second part describes Kalman filter. The third part describes Hardware in Loop Simulation method and its realization using multifunction card MF 624. In the last section of the paper, simulation results are shown for different changes of the induction motor speed which confirm high dynamic properties of the induction motor drive with sensorless control.*

Keywords

Hardware in loop simulation, induction motor, Kalman filter, model reference adaptive system, sensorless control.

1. Introduction

Currently, high attention is paid to a sensorless control of the AC machines whose basic advantages such as a reduction of hardware complexity and cost, increasing mechanical robustness, higher reliability, lower maintenance demands and cost, working in hostile environments, etc., led to the development of different sensorless methods for rotor position and mechanical speed estimation of electrical drives with the induction motors [1], [2].

The sensorless control methods can be classified as follows: a) methods with machine model, b) methods without machine model.

The machine model with higher complexity allows estimating the rotor speed with the sufficient accuracy and is less depending to parameters changes of the induction machine, but also the model reference adaptive system (MRAS) can be used because of its simple implementation in the microcomputer control system. There are various modifications of the model reference adaptive system [3], [4]. The paper is one of the possibilities of the sensorless control and shows the basic theoretical assumptions of the used method.

2. List of the Used Symbols

$\mathbf{\Psi}_r^S$ — rotor flux vector in $[\alpha, \beta]$ coordinate system

$\boldsymbol{u}_S^S$ — stator voltage vector in $[\alpha, \beta]$ coordinate system

$\boldsymbol{i}_S^S$ — stator current vector in $[\alpha, \beta]$ coordinate system

i_{Sx} — magnetizing component of stator current vector

i_{Sy} — torque component of stator current vector

i_m — magnetizing current

R_s, R_r — stator and rotor resistance

L_s, L_r — stator and rotor inductance

L_h — magnetizing inductance

T_r — rotor time constant

T — sampling period

$\Phi(e)$ — adaptation signal

$K_{1,2}$ — PI-controller constants

$\hat{\omega}_m$ — estimated rotor angular speed

3. Observer with Model Reference Adaptive System

The structure of the MRAS observer with Kalman filter is shown in Fig. 1. In this system, induction motor state variables are evaluated in the reference model based on the measured variables (stator voltages, stator currents).

The reference model is independent of the induction motor speed and uses the voltage machine model. The adaptive model uses the current model of the machine and the mechanical angular speed of the machine is one

of the input variables of this model. The difference between state variables is adaptive signal (AS) $\Phi(e)$ which is evaluated and minimized by the PI regulator in the block adaptation mechanism which performs the estimate value of the mechanical angular velocity $\hat{\omega}_m$ and adapts adaptive model until the desired behavior. With feedback, the observer is able to limit the impact of changes in machine parameters to the accuracy of the calculation.
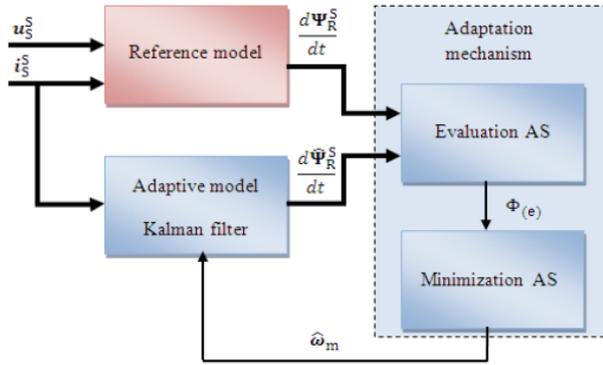
Fig. 1: MRAS with Kalman filter- basic scheme for the estimation of mechanical angular velocity.

3.1. Mathematical Description RF-MRAS

Reference frame MRAS (RF-MRAS) is the simplest variant of observers working on the principle of MRAS. For the estimation, equations are used which determine derivation of the rotor flux of the machine [4].

The reference model of MRAS method is based on the application of voltage model with derivation of the rotor flux which is in the stator coordinate system described by the following equation:

$$\frac{d\boldsymbol{\Psi}_r^S}{dt} = \frac{L_r}{L_h}\left[\boldsymbol{u}_S^S - R_S \boldsymbol{i}_S^S - \frac{L_S L_r - L_h^2}{L_r}\frac{d i_S^S}{dt}\right]. \quad (1)$$

We can express Eq. (1) to the component form:.

$$\frac{d\Psi_{r\alpha}}{dt} = \frac{L_r}{L_h}\left[u_{S\alpha} - R_S i_{S\alpha} - \frac{L_S L_r - L_h^2}{L_r}\frac{d i_{S\alpha}}{dt}\right], \quad (2)$$

$$\frac{d\Psi_{r\beta}}{dt} = \frac{L_r}{L_h}\left[u_{S\beta} - R_S i_{S\beta} - \frac{L_S L_r - L_h^2}{L_r}\frac{d i_{S\beta}}{dt}\right]. \quad (3)$$

The adaptive model of the MRAS method with Kalman filter is based on the application of the current model with derivation of rotor flux, which is in the stator coordinate system described by the following Eq. (4), which depends on the mechanical angular velocity.

$$\frac{d\hat{\boldsymbol{\Psi}}_r^S}{dt} = \left(j\hat{\omega}_m - \frac{1}{T_r}\right)\hat{\boldsymbol{\Psi}}_r^S + \frac{1}{T_r}L_h i_S^S. \quad (4)$$

Equation (4) can be written in component form:

$$\frac{d\hat{\Psi}_{r\alpha}}{dt} = -\frac{1}{T_r}\hat{\Psi}_{r\alpha} - \hat{\omega}_m\hat{\Psi}_{r\beta} + \frac{1}{T_r}L_h i_{S\alpha}, \quad (5)$$

$$\frac{d\hat{\Psi}_{r\beta}}{dt} = -\frac{1}{T_r}\hat{\Psi}_{r\beta} - \hat{\omega}_m\hat{\Psi}_{r\alpha} + \frac{1}{T_r}L_h i_{S\beta}. \quad (6)$$

The error signal entering to the controller is corresponding to the deviation of the rotor flux and it is described by Eq. (7), after processing by PI controller, we get an estimate angular speed ω_m on the output of adaptation algorithm - Eq. (8).

$$\Phi(e) = \frac{d\hat{\Psi}_{r\alpha}}{dt}\frac{d\hat{\Psi}_{r\beta}}{dt} - \frac{d\hat{\Psi}_{r\beta}}{dt}\frac{d\hat{\Psi}_{r\alpha}}{dt}, \quad (7)$$

$$\hat{\omega}_m = K_1\Phi(e) + K_2\int_0^t \Phi(e)dt. \quad (8)$$

Equation (7) corresponds to the opening angle of both vectors. The sign of the error signal $\Phi(e)$ then determines the type of request to change speed. Positive error $\Phi(e) > 0$ requires an increase of the estimated speed and negative error $\Phi(e) < 0$ requires reduction of the estimated speed.

4. Description of Kalman Filter

The Kalman filter is an adaptive filter used to model the states of discrete dynamic system. This technique was developed to filter noise in electrical signals, but later found application in other areas.

The advantage of this filter is its recursive structure, in which the coefficients in each step are adjusted on the basis of available information to provide the best estimate of a future state. The new filter at every step of the filter correction arises from the previous step by the new incoming information without having to remember all previous values of input parameters. With the Kalman filter, we can use the state representation which allows us to create higher order systems working simultaneously as a system of mutually coupled systems of the first order [5], [6], [7], [8], [9].

The Kalman filter allows to obtain no measured state variables (components of rotor flux vector $\Psi_{r\alpha}, \Psi_{r\alpha}$) using measured state variables (components of stator current space vector $i_{S\alpha}, i_{S\beta}$) and also statistics of noise and measurements (covariance matrix of the state vector P, covariance matrix of the system noise vector Q, covariance matrix of the measurement noise vector R).

The general model of the controlled system in discrete form can be written as:

$$\boldsymbol{x}(t+T) = \boldsymbol{A}\boldsymbol{x}(t) + \boldsymbol{B}\boldsymbol{u}(t) + \boldsymbol{w}(t). \quad (9)$$

Measurement model provides prediction of measurement:

$$\boldsymbol{y}(t) = \boldsymbol{C}\boldsymbol{x}(t) + \boldsymbol{v}(t). \tag{10}$$

The notation of matrices in discrete form, which include an influence of the sampling period T, is following: **A**-state matrix, **B**-matrix of inputs, **C**-matrix of outputs. Matrix **C** defines measurement relations to the state variable **x**.

The system noise **w** has a covariance matrix **Q** and the measurement noise **v** has a covariance matrix **R**, which characterize the uncertainties in the states and correlations within it.

The state covariance matrix **P** is obtained in prediction part of the algorithm. After fulfillment actual measurement, it is then corrected. The covariance matrices **Q**, **R** is necessary experimentally set up.

4.1. Method of Calculation

We can define state equations and measurement equations as follows:

Improvement = measured value - prediction:

$$\boldsymbol{z}(t) = \boldsymbol{y}(t) - \boldsymbol{H}\tilde{\boldsymbol{x}}(t), \tag{11}$$

$$\boldsymbol{H} = \begin{bmatrix} 1 & 0 \end{bmatrix}. \tag{12}$$

Estimation of state:

$$\hat{\boldsymbol{x}}(t) = \tilde{\boldsymbol{x}}(t) + \boldsymbol{K}(t)\boldsymbol{z}(t). \tag{13}$$

Prediction of state:

$$\tilde{\boldsymbol{x}}(t + T) = \boldsymbol{A}\hat{\boldsymbol{x}}(t). \tag{14}$$

We can define Kalman gain and error covariance equations as follows:

Kalman gain:

$$\boldsymbol{K}(t) = \tilde{\boldsymbol{P}}(t)\boldsymbol{H}^T \left(\boldsymbol{H}\tilde{\boldsymbol{P}}(t)\boldsymbol{H}^T + \boldsymbol{R} \right)^{-1}. \tag{15}$$

Estimation of the covariance matrix:

$$\hat{\boldsymbol{P}}(t) = \left[\boldsymbol{I} - \boldsymbol{K}(t)\boldsymbol{H} \right] \tilde{\boldsymbol{P}}(t). \tag{16}$$

Prediction covariance matrix:

$$\tilde{\boldsymbol{P}}(t) = \boldsymbol{A}\hat{\boldsymbol{P}}(t + T)\boldsymbol{A}^T + \boldsymbol{Q}. \tag{17}$$

5. Description of HIL Method

Hardware in the Loop (HIL) simulation is a technique that is used in the development and testing of complex real-time systems. It is a tool that connects the hardware (controller) with a mathematical model (managed system) in a closed feedback loop. To simulate this method a real control system and a mathematical model is required.

The mathematical model is used to configure the control system. The control system generates an actuator variable dependent on the control deviation, which is the difference between desired and actual quantity. The control variable enters the model, and then output variable (actual value) gets off from the mathematical model, and then gets back in to the control system.
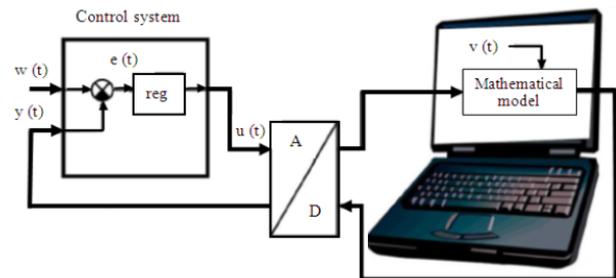
Fig. 2: Diagram of hardware in the loop simulation.

The HIL simulation works in real time. Results of this simulation approach to reality, because the control system with sensors and actuators is implemented as close as it would be in real. To the fact that the results would match the reality, we need a sufficiently accurate mathematical model, on which simulation accuracy dependents most. As soon as the control system is set up according to the requirements, a mathematical model can be replaced by the real system and the results can be compared.

Figure 2 shows a general diagram of the HIL simulation. The meaning of quantities in this figure is following: $y(t)$ - process value, $w(t)$ - reference quantity, $e(t)$ - control error, $u(t)$ - control quantity, $v(t)$ - fault quantity, reg - regulator, A/D - A/D and D/A converters.

5.1. Description of Multifunction Card

MF 624 multifunction I/O card is designed for the needs of connection a PC compatible computer to the real signals from outside the world. MF 624 contains a fast 8-channel 14-bit A/D converter with simultaneous sampling of multiple channels and function of storage measured values from the A/D conversion, 8 independent 14-bit D/A converter, 8-bit digital inputs, 8-bit digital outputs and quintuple timer/counter. The card is designed for standard data acquisition and control applications and is optimized for use with the Real Time Toolbox for Simulink. MF 624 offers full 32-
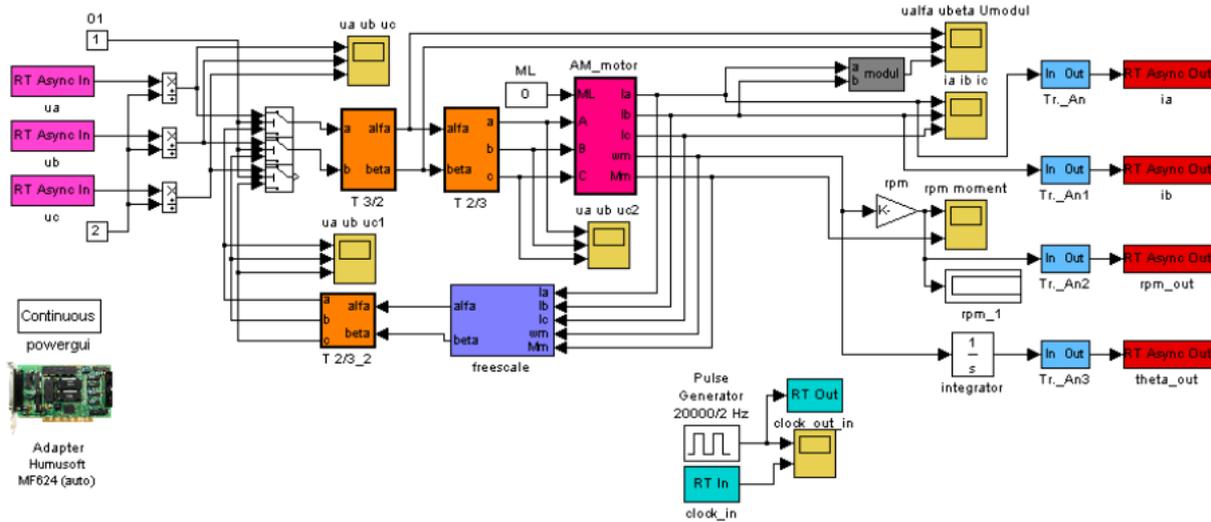
Fig. 3: Induction motor in the simulated model - Matlab-Simulink.

bit architecture for fast data processing. Multifunction I/O Card MF 624 can be installed in any available PCI slot.

5.2. Multifunction Card Connection to PC

Multifunction Card MF 624 is a device that communicates with the PC through software Real Time Toolbox. This toolbox is installed as an additional part of the Matlab-Simulink. The mathematical model representing the controlled system runs in Matlab-Simulink environment. Real Time Toolbox is a package to connect Simulink to the real world. It acquires data in real time, they are immediately processed by a mathematical model in Simulink and the results are sent back to the outside world. Real Time Toolbox contains a library of blocks for input and output support in real time. All functions are implemented as Simulink blocks with a standard graphical interface, which allows both: an easy start for beginners and high productivity of experienced users. The parts of the toolbox are demonstration examples of basic systems.

5.3. Realized Connection with HIL Method

Custom hardware testing methods in the Loop Simulation were performed on the vector control of asynchronous motor (AM). AM model was compiled according to differential equations in Matlab-Simulink. Communication model AM is realized through analog and digital input - output blocks from the library of the Real Time Toolbox. Figure 3 shows the diagram of the simulated model AM in Matlab, Simulink, in-

cluding I/O blocks. The control system, respectively the real world is made by MC56F8037 microcontroller, which is connected to the multifunction card MF 624.

Communication is solved by an A/D and D/A converters, whose are brought from the PC via data cable with terminal block connection which allows connection of another electronic devices. Concretely, in this connection there are in the output of D/A converters voltages proportional to the phase currents ia and ib, then an analog value of rotor position and an analog value of the motor speed. On the contrary, the input A/D converters are through the RC-filter connected to the microcontroller MC56F8037 PWM output.

These stator voltages are proportional to the desired voltages ua and ub. RC filters are used in order to accelerate the simulation. Analog voltage proportional to the desired voltages ua and ub is then converted by Matlab to PWM signals. This conversion is realized by comparison of signal and saw the signal at frequency 2 kHz.

Control variables of vector control, i.e. the reference speed and the reference magnetizing current, are entered in LabVIEW program which is connected to Microcontroller MC56F8037 through USB data cable. This program can run on another PC or together on PC with the original MATLAB. In addition to setting control variables of vector control, this program shows the process of selected variables vector [10].

6. Simulation Result

In this chapter, simulation results of sensorless vector control of the induction motor are shown which were recorded by the program for setting control variables in

LabVIEW environment. The reference speed has the value at first 30 rpm, respectively 300 rpm, and then was changed to -30 rpm, respectively -300 rpm. Meaning individual variables is obvious from the description of figures.
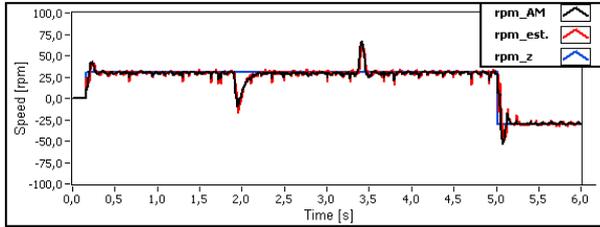
Fig. 4: Change of the motor speed [rpm] from $0\ rpm\ \rightarrow$ $30\ rpm \rightarrow -30\ rpm$, the actual speed (black), estimated speed (red), reference speed (blue).
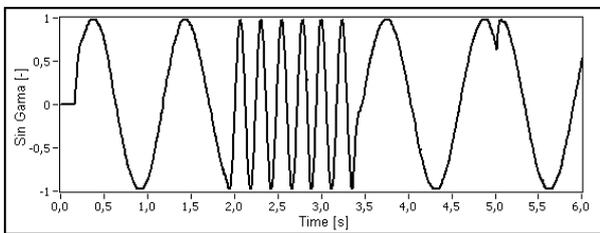
Fig. 5: Sin function of orienting angle $sin\gamma$ $[-]$.
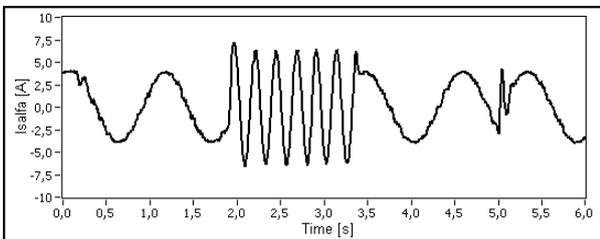
Fig. 6: Stator current $i_{S\alpha}$ $[A]$.
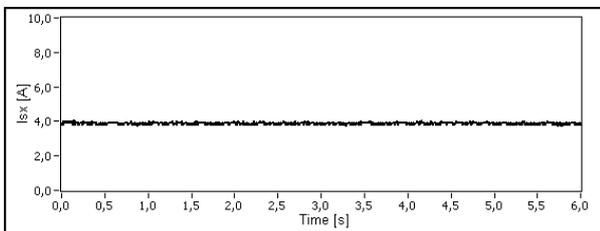
Fig. 7: Magnetizing component of stator current vector i_{Sx} $[A]$.

The simulation results confirm very good dynamic responses of controlled quantities. Presented speed estimator is suitable for the sensorless control of the IM also in the area of the very low speed about 10 rpm.
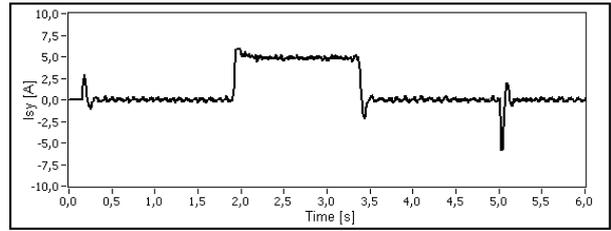
Fig. 8: Torque component of stator current vector i_{Sy} $[A]$.
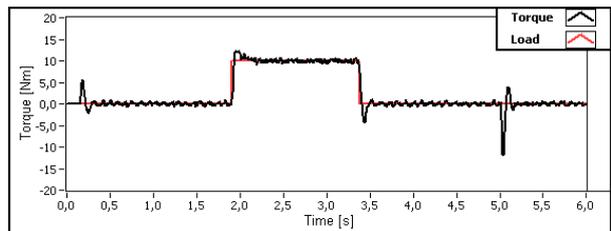
Fig. 9: Torque of the IM [Nm] (black), load torque [Nm] (red).
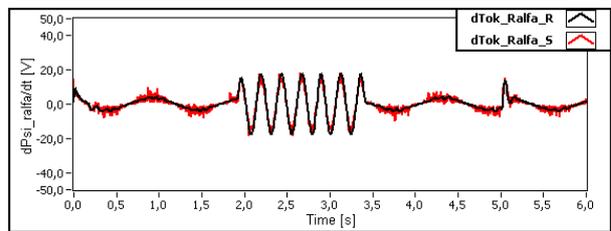
Fig. 10: Rotor flux derivative $d\Psi_{r\alpha}/dt$ $[V]$, the current model (black), the voltage model (red).
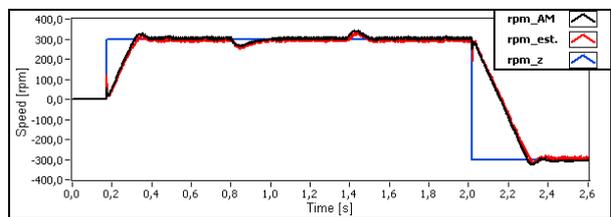
Fig. 11: Change of the motor speed [rpm] from $0\ rpm\ \rightarrow$ $300\ rpm \rightarrow -300\ rpm$, the actual speed (black), estimated speed (red), reference speed (blue).
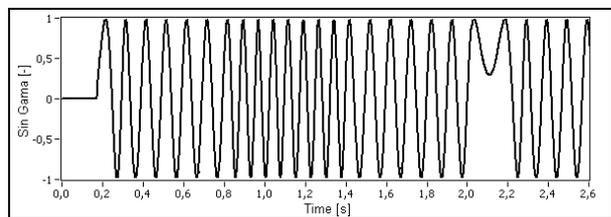
Fig. 12: Sin function of orienting angle $sin\gamma[-]$.

7. Conclusion

The estimation technique for sensorless induction motor drive with vector control was presented in the pa-
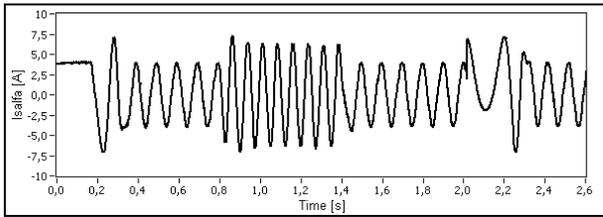
Fig. 13: Stator current $i_{S\alpha}$ [A].
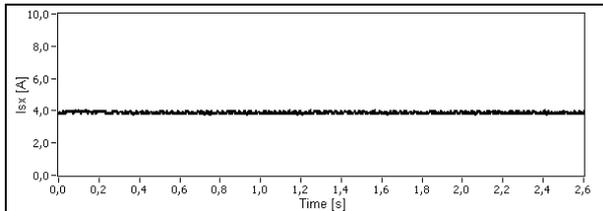
Fig. 14: Magnetizing component of stator current vector i_{Sx} [A].
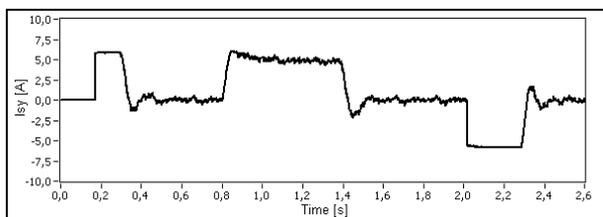
Fig. 15: Torque component of stator current vector i_{Sy} [A].
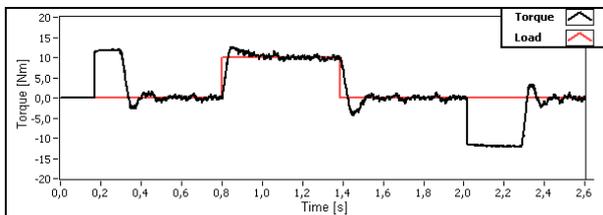
Fig. 16: Torque of the IM [Nm] (black), load torque [Nm] (red).
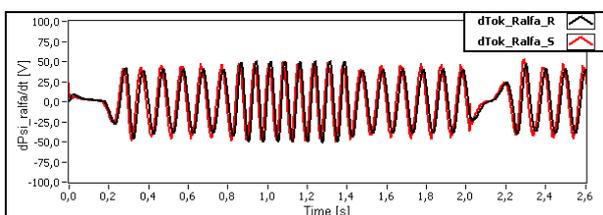
Fig. 17: Rotor flux derivative $d\Psi_{r\alpha}/dt$ [V], the current model (black), the voltage model (red).

per. The speed estimator is based on application of the Model Reference Adaptive System with Kalman filter.

The sensorless induction motor drive with the presented speed estimator gives good dynamic responses also in the area of the very low speed. The estimation of the mechanical speed is good in steady state and also in transient state. To select an appropriate

method for sensorless control of the induction motor, it is necessary to define the basic requirements, for example the speed control range, the accuracy of speed or rotor position evaluation, the activity in continuous mode or as a substitution in case of damaged sensors, etc.

The simulation results which were obtained using HIL method show that the method is suitable for use in research and testing modern control methods of electrical drives without the direct use of the real motor and frequency converter.

Acknowledgment

References

[1] HOLTZ J. Sensorless Control of Induction Motor Drives. *Proceedings of the IEEE.* 2002, vol. 90, iss. 8, pp. 1359-1394. ISSN 0018-9219. DOI: 10.1109/JPROC.2002.800726.

[2] LASCU Ch., I. BOLDEA and F. BLAAB-JERG. Comparative Study of Adaptive and Inherently Sensorless Observers for Variable-Speed Induction-Motor Drives. *IEEE Transactions on Industrial Electronics.* 2006, vol. 53, iss. 1, pp. 57-65. ISSN 0278-0046. DOI: 10.1109/TIE.2005.862314.

[3] BELLINI A. and S.BIFARETTI. Sensitivity to Parameters' Variations in Sensorless Induction Motor Drives Using a Reduced Order MRAS Observer. *International Review of Electrical Engineering - IREE.* 2007, vol. 2, no. 2, pp. 242-249. ISSN 1827-6660.

[4] BRANDSTETTER P. Sensorless Control of Induction Motor Using Modified MRAS. *International Review of Electrical Engineering - IREE.* 2012, vol. 7, no. 3, pp. 4404-4411, 2012. ISSN 1827-6660.

[5] SALVATORE N., A. CAPONIO, F. NERI, S. STASI and G. L. CASCELLA. Optimization of Delayed-State Kalman-Filter-Based Algorithm via Differential Evolution for Sensorless Control of

Induction Motors. *IEEE Transactions on Industrial Electronics*. 2010, vol. 57, iss. 1, pp. 385 - 394. ISSN 0278-0046. DOI: 10.1109/TIE.2009.2033489.

[6] HENNEBERGER G., B. J. BRUNSBACH and T. KLEPSCH. Field Oriented Control of Synchronous and Asynchronous Drives without Mechanical Sensors Using a Kalman-Filter. In: *European Conference on Power Electronics and Applications EPE*. Florence: IEEE, 1991, vol. 3, pp. 664-671.

[7] KIM, Y. R., S. K. SUL and M. H. PARK. Speed Sensorless Vector Control of Induction Motor Using Extended Kalman Filter. *IEEE Transactions on Industry Applications*. 1994, vol. 30, iss. 5, pp. 1225-1233. ISSN 00939994. DOI: 10.1109/28.315233.

[8] SMIDL, V. and Z. PEROUTKA. Advantages of Square-Root Extended Kalman Filter for Sensorless Control of AC Drives. *IEEE Transactions on Industrial Electronics*. 2012, vol. 59, iss. 11, pp. 4189-4196. ISSN 0278-0046. DOI: 10.1109/TIE.2011.2180273.

[9] SUTNAR, Z., Z. PEROUTKA and M. RODIC. Comparison of Sliding Mode Observer and Extended Kalman Filter for Sensorless DTC-Controlled Induction Motor Drive. In: *Proc. of the 14th International Power Electronics and Motion Control Conference (EPE/PEMC)*. Ohrid: IEEE, 2010, pp. T7−55−T7−62. ISBN 978-1-4244-7856-9. DOI: 10.1109/EPEPEMC.2010.5606844.

[10] SLIVKA, D., P. PALACKY, P. VACULIK and A. HAVEL. Electric Vehicle Control Units Communication. *Advances in Electrical and Electronic Engineering*. 2012, vol. 10, no. 1, pp. 17-21. ISSN 1804-3119.

About Authors

Pavel BRANDSTETTER was born in Ostrava, Czech Republic, 1955, 1 June. He received the M.Sc. and Ph.D. degrees in Electrical Engineering from Brno University of Technology, Czech Republic, in 1979 and 1987, respectively. He is currently full professor in Electrical Machines, Apparatus and Drives and vice dean of Faculty of Electrical Engineering and Computer Science at VSB–Technical University of Ostrava. His current research interests are applied electronics, power semiconductor systems, microcomputer control systems and modern control methods of electrical drives.

Marek BOBROVSKY was born in Ostrava, Czech Republic, 1978, 23 August. He obtained Master's degree in field of Electronics in 2009 at VSB–Technical University of Ostrava. He is currently Ph.D. student at Department of Electronics, Faculty of Electrical Engineering and Computer Science. His research area includes microcomputer control systems and modern control methods of electrical drives.